

Compressive sampling based MVDR spectrum sensing

Ying Wang*[†], Ashish Pandharipande* and Geert Leus[†]

*Philips Research Europe,

High Tech Campus, 5656 AE Eindhoven, The Netherlands

Email: {ying.z.wang, ashish.p}@philips.com

[†]Department of EEMCS, Delft University of Technology, The Netherlands

Email: g.j.t.leus@tudelft.nl

Abstract—We propose a compressive sampling (CS) based MVDR spectrum estimator, which estimates the wideband spectrum from the compressed signals with sub-Nyquist-rate sampling. To analyze detection performance, we derive the statistics of the estimated CS MVDR spectrum considering finite samples. We also show that different compression matrices produce different levels of signal leakage and influence the computation of detection thresholds.

I. INTRODUCTION

Large portions of spectrum in the VHF-UHF bands are under-utilized, and regulatory activities are ongoing for permitting secondary usage of such bands [5]. Cognitive radios enable us to improve the spectral utilization via spectrum sensing. The idea is to determine frequency bands free of signal transmissions from licensed users or primary users, so that such bands can be used by secondary users opportunistically. One key challenge of spectrum sensing is the large bandwidth of interest, e.g. a few GHz. This imposes impractical burden on the conventional analog-to-digital convertors (ADC) with Nyquist-rate sampling.

Compressive sampling (CS) is a method of acquisition and reconstruction of sparse signals [4]. One application of CS is the analog-to-information convertor (AIC) that can sample below the Nyquist-rate [7]. By exploiting the fact that the spectrum is under-utilized and therefore sparse, we can reconstruct the original wideband spectrum from the compressed signal (acquired by e.g., an AIC), using well-known approaches like l_1 -norm minimization [4].

The CS reconstruction based spectrum estimation usually involves iterative algorithms with high complexity [3], as compared to the conventional spectrum estimation like periodogram. The minimum variance distortionless response (MVDR) estimator, also known as Capon beamformer [1], was originally proposed for array-based high resolution angle spectrum estimation. An CS array architecture proposed in [10] illustrates that the estimated angle spectrum using the CS MVDR approach is reasonably well comparing to that using the CS reconstruction approach.

In this paper, we propose a CS MVDR approach for wideband spectrum sensing, with much less computational complexity than commonly used CS reconstruction algorithms. The analog wideband signal is first sampled by a sub-Nyquist-

rate AIC. Then the wideband spectrum is estimated from the compressed signal using the proposed CS MVDR estimator. A Neyman-Pearson detector is applied on the estimated spectrum to determine for each frequency bin whether some primary signal is present or not.

II. SIGNAL MODEL

The time domain signal is divided into blocks of equal length. Each block contains N discrete time samples at Nyquist-rate sampling. Taking an N_s -point ($N_s \geq N$) Discrete Fourier Transform (DFT) on one block of time samples (with zero-padding if needed), we obtain the frequency domain signal of length N_s . We will refer to one block as one snapshot. Let $t = 1, 2, \dots, Q$ denote the snapshot index, Q being the total number of snapshots. The received time domain signal at the t -th snapshot can be written as

$$\mathbf{x}_t = \mathbf{\Psi}_x \mathbf{z}_t + \mathbf{n}_t, \quad (1)$$

where $\mathbf{\Psi}_x$ is an $N \times N_s$ basis matrix, \mathbf{z}_t is an $N_s \times 1$ vector of frequency domain signals without noise, and \mathbf{n}_t is an $N \times 1$ vector of additive white Gaussian noise (AWGN) with variance σ_n^2 . The basis matrix $\mathbf{\Psi}_x$ consists of N_s basis vectors, i.e.,

$$\mathbf{\Psi}_x = [\mathbf{a}(\omega_1) \ \mathbf{a}(\omega_2) \ \dots \ \mathbf{a}(\omega_{N_s})]. \quad (2)$$

Each basis vector $\mathbf{a}(\omega_i)$ is a complex exponential sequence with frequency ω_i , i.e.,

$$\mathbf{a}(\omega_i) = [1 \ e^{j\omega_i} \ \dots \ e^{j\omega_i(N-1)}]^T / \sqrt{N}, \quad (3)$$

$$\omega_i = 2\pi i / N_s, \quad i = 1, 2, \dots, N_s.$$

Note that

$$\mathbf{\Psi}_x^H = \bar{\mathbf{F}}_{N_s}, \quad (4)$$

where $\bar{\mathbf{F}}_{N_s}$ is the first N columns of an $N_s \times N_s$ normalized DFT matrix \mathbf{F}_{N_s} (whose column norm is N_s/N).

We sample the received signal using an AIC and obtain the CS measurement signal \mathbf{y}_t . The relationship between the original Nyquist-rate signal \mathbf{x}_t of (1) and \mathbf{y}_t is

$$\mathbf{y}_t = \mathbf{\Phi} \mathbf{x}_t = \mathbf{\Phi} \mathbf{\Psi}_x \mathbf{z}_t + \mathbf{\Phi} \mathbf{n}_t = \mathbf{\Psi}_y \mathbf{z}_t + \mathbf{m}_t, \quad (5)$$

where $\mathbf{\Phi}$ is a CS measurement matrix of size $M \times N$ ($M < N$). Here we use discrete-time representations for both \mathbf{x}_t and

\mathbf{y}_t , by viewing the AIC conceptually as a Nyquist-rate ADC followed by a compression matrix Φ . In practice, the AIC operates on the analog version of \mathbf{x}_t and outputs the digital signal \mathbf{y}_t , where the multiplication with the matrix Φ can be implemented using mixers and integrators [7]. The covariance matrix of the CS measurement signal is defined by

$$\mathbf{R}_y = E[\mathbf{y}_t \mathbf{y}_t^H] = \Psi_y \mathbf{R}_z \Psi_y^H + \mathbf{R}_m, \quad (6)$$

where $E[\cdot]$ is the expectation operator, $\Psi_y = \Phi \Psi_x$ is the basis matrix of the compressed signal, and \mathbf{R}_z , \mathbf{R}_m are the covariance matrices defined respectively by

$$\mathbf{R}_z = E[\mathbf{z}_t \mathbf{z}_t^H] = \text{diag}[\sigma_1^2 \ \sigma_2^2 \ \cdots \ \sigma_{N_s}^2], \quad (7)$$

$$\mathbf{R}_m = E[\mathbf{m}_t \mathbf{m}_t^H] = \sigma_n^2 \Phi \Phi^H. \quad (8)$$

In (7) we assume that the frequency domain signal vector \mathbf{z}_t contains N_s uncorrelated coefficients with zero mean and variances σ_i^2 , $i = 1, 2, \dots, N_s$. In wideband spectrum estimation, the signal is assumed to be sparse in frequency domain, i.e., the $N_s \times 1$ vector \mathbf{z}_t has only K ($K \ll N$) nonzero coefficients. Let $\Omega = \{\omega_i | i = i_1, i_2, \dots, i_K\}$ be a set of active frequencies occupied by signals, and $\bar{\Omega}$ be the remaining $N_s - K$ frequencies occupied by noise only. If we denote the i -th element of \mathbf{z}_t as $z_t(\omega_i)$, then $z_t(\omega_i)$ is nonzero at frequencies $\omega_i \in \Omega$, and zeros otherwise.

III. PROBABILITY DISTRIBUTION OF THE CS MVDR SPECTRUM ESTIMATE

Based on the CS measurement signal of (5), we obtain the CS MVDR spectrum given by

$$P_y(\omega_i) = \frac{1}{\mathbf{b}(\omega_i)^H \mathbf{R}_y^{-1} \mathbf{b}(\omega_i)}, \quad i = 1, 2, \dots, N_s, \quad (9)$$

where $\mathbf{b}(\omega_i) = \Phi \mathbf{a}(\omega_i)$ is a basis vector in Ψ_y . When we have only Q snapshots available, a sample covariance matrix is calculated by

$$\hat{\mathbf{R}}_y = (\mathbf{Y} \mathbf{Y}^H) / Q, \quad (10)$$

and the CS MVDR spectrum estimate with finite snapshots is

$$\hat{P}_y(\omega_i) = \frac{1}{\mathbf{b}(\omega_i)^H \hat{\mathbf{R}}_y^{-1} \mathbf{b}(\omega_i)}. \quad (11)$$

Since \mathbf{x}_t is an N -variate complex Gaussian random variable and \mathbf{y}_t is an M -variate complex Gaussian random variable, the sample covariance matrix $\hat{\mathbf{R}}_y$ of (10) follows a complex Wishart distribution [6]. Extending the result of [9, Theorem 3.4.7] to the complex-valued case, we have

$$\frac{1}{\mathbf{b}^H \hat{\mathbf{R}}_y^{-1} \mathbf{b}} \sim \frac{1}{2Q} \frac{1}{\mathbf{b}^H \mathbf{R}_y^{-1} \mathbf{b}} \chi_{2(Q-M+1)}^2, \quad (12)$$

i.e., $\hat{P}_y(\omega_i) \sim \frac{1}{2Q} P_y(\omega_i) \chi_{2(Q-M+1)}^2$,

where χ_v^2 denotes a centralized Chi-square distribution with v degrees of freedom, and for simplicity of notation we omitted the parameter ω_i of the basis vector $\mathbf{b}(\omega_i)$. The finite snapshots based MVDR spectrum estimate is a Chi-square

random variable multiplied by the true MVDR spectrum (with a scaling factor), with mean and variance given by

$$\begin{aligned} E[\hat{P}_y(\omega_i)] &= P_y(\omega_i)(Q - M + 1)/Q \\ \text{Var}[\hat{P}_y(\omega_i)] &= P_y^2(\omega_i)(Q - M + 1)/Q^2. \end{aligned}$$

The probability distribution of $\hat{P}_y(\omega_i)$ is needed to determine the presence of signals at frequency ω_i .

IV. SIGNAL DETECTION

Using the estimated CS MVDR spectrum $\hat{P}_y(\omega_i)$, the detection problem is to determine for each frequency ω_i whether some primary signal is present or not. Following the Neyman-Pearson approach, we compare $\hat{P}_y(\omega_i)$ with a threshold $\gamma(\omega_i)$ to distinguish between two hypotheses:

$$\hat{P}_y(\omega_i) \begin{cases} \geq \gamma(\omega_i) & \mathcal{H}_1 : \text{signal present, i.e., } \omega_i \in \Omega \\ < \gamma(\omega_i) & \mathcal{H}_0 : \text{signal absent, i.e., } \omega_i \in \bar{\Omega}. \end{cases} \quad (13)$$

We wrote the threshold as $\gamma(\omega_i)$ since it may depend on the frequency ω_i . To design a threshold we need to know the distribution of $\hat{P}_y(\omega_i)$ at noise only frequencies $\omega_i \in \bar{\Omega}$. This distribution is given by (12) and it requires the knowledge of the true CS MVDR spectrum, i.e., $P_y(\omega_i)$ at $\omega_i \in \bar{\Omega}$. It is desired that the threshold is independent of the primary signals, which is possible only if there is no signal leakage to the noise-only frequencies, i.e., $P_y(\omega_i)$ does not contain signal contribution at $\omega_i \in \bar{\Omega}$.

A. Signal leakage of the CS MVDR spectrum

To analyze the signal leakage effects, we first define an $N_s \times N_s$ matrix \mathbf{P}_y as

$$\mathbf{P}_y = \Psi_y^H \mathbf{R}_y^{-1} \Psi_y. \quad (14)$$

Applying the *matrix inversion lemma* [8] on (6), \mathbf{R}_y^{-1} becomes

$$\mathbf{R}_y^{-1} = \mathbf{R}_m^{-1} - \mathbf{R}_m^{-1} \Psi_y (\mathbf{R}_z^{-1} + \Psi_y^H \mathbf{R}_m^{-1} \Psi_y)^{-1} \Psi_y^H \mathbf{R}_m^{-1}. \quad (15)$$

Then \mathbf{P}_y of (14) can be expressed by a noise-only matrix \mathbf{P}_m and a signal dependent matrix \mathbf{P}_s :

$$\mathbf{P}_y = \mathbf{P}_m - \mathbf{P}_s, \quad (16)$$

$$\mathbf{P}_m = \Psi_y^H \mathbf{R}_m^{-1} \Psi_y = \sigma_n^{-2} \Psi_x^H \mathbf{P}_\Phi \Psi_x, \quad (17)$$

$$\mathbf{P}_s = \mathbf{P}_m \mathbf{R}_z^{1/2} (\mathbf{I} + \mathbf{R}_z^{1/2} \mathbf{P}_m \mathbf{R}_z^{1/2})^{-1} \mathbf{R}_z^{1/2} \mathbf{P}_m, \quad (18)$$

where $\mathbf{P}_\Phi = \Phi^H (\Phi \Phi^H)^{-1} \Phi = \Phi^\dagger \Phi$ is the projection matrix onto the column-space of Φ (\dagger denotes the Moore-Penrose pseudoinverse), and \mathbf{I} is an $N_s \times N_s$ identity matrix. The CS MVDR spectrum of (9) can thus be rewritten as the diagonal elements of \mathbf{P}_y , i.e., for $i = 1, 2, \dots, N_s$,

$$P_y(\omega_i) = \frac{1}{[\mathbf{P}_y]_{i,i}} = \frac{1}{[\mathbf{P}_m]_{i,i} - [\mathbf{P}_s]_{i,i}}. \quad (19)$$

To avoid signal leakage, $[\mathbf{P}_s]_{i,i}$ must contain no signal contribution at noise-only frequencies $\omega_i \in \bar{\Omega}$, which is true only when \mathbf{P}_m is diagonal. If \mathbf{P}_m is banded, i.e., its matrix elements are zero outside a diagonally bordered band, then we have some signal leakage in the neighborhood of active

frequencies $\omega_i \in \Omega$. Whether \mathbf{P}_m is diagonal or banded depends on the following cases:

- 1) Nyquist-rate signals ($M = N$), the compression matrix $\mathbf{\Phi} = \mathbf{I}_N$ and the projection $\mathbf{P}_\Phi = \mathbf{I}_N$. Depending on whether spectral smoothing is used or not, we have

- a) no spectral smoothing ($N = N_s$):

$$\mathbf{P}_m = \sigma_n^{-2} \mathbf{F}_{N_s} \mathbf{F}_{N_s}^H = \sigma_n^{-2} \mathbf{I} = \text{diagonal.}$$

- b) with spectral smoothing ($N < N_s$):

$$\mathbf{P}_m = \sigma_n^{-2} \bar{\mathbf{F}}_{N_s} \bar{\mathbf{F}}_{N_s}^H = \text{well banded.}$$

- 2) Compressed signals ($M < N$), the compression matrix $\mathbf{\Phi}$ contains elements drawn i.i.d. from a random distribution and the $N \times N$ projection \mathbf{P}_Φ has rank M .

- a) no spectral smoothing ($N = N_s$):

$$\mathbf{P}_m = \sigma_n^{-2} \mathbf{F}_{N_s} \mathbf{P}_\Phi \mathbf{F}_{N_s}^H = \text{less banded.}$$

- b) with spectral smoothing ($N < N_s$):

$$\mathbf{P}_m = \sigma_n^{-2} \bar{\mathbf{F}}_{N_s} \mathbf{P}_\Phi \bar{\mathbf{F}}_{N_s}^H = \text{less banded.}$$

For both case 1) and case 2), more spectral smoothing (i.e., larger N_s/N for a fixed N_s) results in a wider diagonal band in \mathbf{P}_m . For case 1) when there is no compression, \mathbf{P}_m is well banded, i.e., its out-of-band power is close to zero. For case 2) when a compression matrix is involved, we say that \mathbf{P}_m is 'less banded' because its out-of-band power is considerably higher than that of case 1). The out-of-band power of \mathbf{P}_m is related to the compression ratio M/N and the type of compression matrix $\mathbf{\Phi}$ used, or more exactly, whether $\mathbf{\Phi}$ has a Toeplitz structure or not. A Toeplitz $\mathbf{\Phi}$ produces a most banded \mathbf{P}_m because the signal basis $\mathbf{\Psi}_x$ has a Fourier structure.

B. Threshold computation

For Nyquist-rate signals, $[\mathbf{P}_m]_{i,i}$ is constant over all the frequencies. For compressed signals, the original white noise is colored by the compression matrix $\mathbf{\Phi}$ and $[\mathbf{P}_m]_{i,i}$ varies over frequencies (except for a random selection $\mathbf{\Phi}$). This suggests a frequency varying threshold. For convenience we can whiten (11) to get an improved CS MVDR spectrum estimate:

$$\tilde{P}_y(\omega_i) = \frac{\mathbf{a}(\omega_i)^H \mathbf{P}_\Phi \mathbf{a}(\omega_i)}{\mathbf{b}(\omega_i)^H \bar{\mathbf{R}}_y^{-1} \mathbf{b}(\omega_i)} = \hat{P}_y(\omega_i) [\mathbf{P}_m]_{i,i} \sigma_n^2, \quad (20)$$

which has a probability distribution of

$$\tilde{P}_y(\omega_i) \sim \frac{\sigma_n^2}{2Q(1 - [\mathbf{P}_s]_{i,i}/[\mathbf{P}_m]_{i,i})} \chi_{2(Q-M+1)}^2 \quad (21)$$

Using the detection approach of (13), for a given threshold γ we can calculate the probability of false alarm as

$$\begin{aligned} p_f &= \text{Prob}\{\tilde{P}_y(\omega_i) > \gamma | \mathcal{H}_0\} \\ &= F_r\left(\frac{2Q\gamma(1 - [\mathbf{P}_s]_{i,i}/[\mathbf{P}_m]_{i,i})}{\sigma_n^2}\right), \quad \omega_i \in \bar{\Omega}, \quad (22) \end{aligned}$$

where $F_r(\cdot)$ is the right-tail integral of the $\chi_{2(Q-M+1)}^2$ distribution. For a given p_f , the threshold can be found by

$$\gamma = \frac{F_r^{-1}(p_f) \sigma_n^2}{2Q(1 - [\mathbf{P}_s]_{i,i}/[\mathbf{P}_m]_{i,i})}, \quad \omega_i \in \bar{\Omega}. \quad (23)$$

For Nyquist-rate signals, when $N_s/N = 1$ the signal leakage term $[\mathbf{P}_s]_{i,i} = 0$ at noise-only frequencies $\omega_i \in \bar{\Omega}$, whereas when $N_s/N > 1$ there will be some signal leakage but negligible. For compressed signals with a Toeplitz compression matrix, the signal leakage only affects the neighborhood of active frequencies, i.e., $[\mathbf{P}_s]_{i,i} \approx 0$ at frequencies $\omega_i \in \bar{\Omega}$, where $\tilde{\Omega} \subset \bar{\Omega}$ denotes the set of noise-only frequencies far away from the active frequencies. Then a threshold for a given p_f is $\gamma = F_r^{-1}(p_f) \sigma_n^2 / (2Q)$. For compressed signals with a non-Toeplitz compression matrix, $[\mathbf{P}_s]_{i,i}$ is not negligible at noise-only frequencies.

V. SIMULATION

We simulate an example scenario of the wideband spectrum with mixed analog/digital broadcasting television transmission. The total bandwidth of interest is 128 MHz, which is also the Nyquist sampling rate. Assume that we have 1 ms of signal available for spectrum sensing. The total number of Nyquist-rate samples is 128000. The number of frequencies is $N_s = 256$, which corresponds to a frequency resolution of 0.5 MHz. The primary signals consist of two digital TV transmissions (each occupying 16 frequencies, i.e. 8 MHz bandwidth) and 4 analog TV transmissions (each occupying a single frequency). The number of active frequencies is $K = 36$. The noise power is $\sigma_n^2 = 1$. The signals at active frequencies are generated using random bits with binary phase shift keying (BPSK) modulation. The signal power σ_i^2 is equal for all the active frequencies $\omega_i \in \Omega$, and the signal-to-noise (SNR) ratio is defined by σ_i^2/σ_n^2 . The compression ratio is $M/N = 0.3$. If $N = N_s$ (no spectral smoothing), then $M = 77$ and $Q = 500$. If $N = N_s/2$ (with spectral smoothing), then $M = 38$ and $Q = 1000$. With a fixed compression ratio, a larger pair of M and N results in more complexity in the AIC implementation and the spectrum estimation.

We consider three different compression matrices: 1) 'randn' - general random Gaussian $\mathbf{\Phi}$, whose elements are drawn i.i.d. from a random Gaussian distribution of zero mean and variance $1/M$; 2) 'toeprnc' - Toeplitz random Gaussian $\mathbf{\Phi}$, whose elements are drawn from the same distribution as in 1) and with a Toeplitz structure; 3) 'rande' - random selection $\mathbf{\Phi}$, which is constructed by randomly selecting M columns from an $N \times N$ identity matrix and multiplied with a normalization factor $\sqrt{N/M}$.

We first show how banded the matrix \mathbf{P}_m of (17) is under different situations. The more banded the \mathbf{P}_m is (i.e., more close to a diagonal matrix), the less signal leakage to the noise-only frequencies. We plot the amplitude of \mathbf{P}_m for different compression matrices $\mathbf{\Phi}$. Figure 1 shows the $|\mathbf{P}_m|$ in linear scale for a $\mathbf{\Phi}$ equal to the identity matrix (i.e., no compression), which gives a diagonal \mathbf{P}_m (when $N_s/N = 1$) and a well banded \mathbf{P}_m (when $N_s/N = 2$). Figures 2, 3 and 4 show the $|\mathbf{P}_m|$ in dB scale for a Toeplitz random Gaussian $\mathbf{\Phi}$, a general random Gaussian $\mathbf{\Phi}$, and a random selection $\mathbf{\Phi}$, respectively. We can see that a Toeplitz $\mathbf{\Phi}$ produces a most banded \mathbf{P}_m , which has its diagonal-band elements about 30 dB higher than the rest of the elements. For non-Toeplitz $\mathbf{\Phi}$'s,

the diagonal-band elements are about 15 dB higher than the rest of the elements of \mathbf{P}_m .

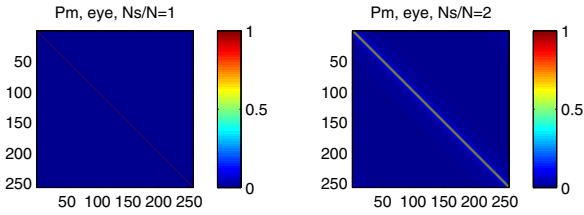


Fig. 1. $|\mathbf{P}_m|$ (in linear scale) for $\Phi = \mathbf{I}_N$ (no compression).

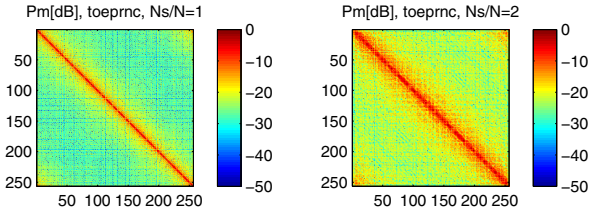


Fig. 2. $|\mathbf{P}_m|$ (in dB) for a Toeplitz random Gaussian Φ .

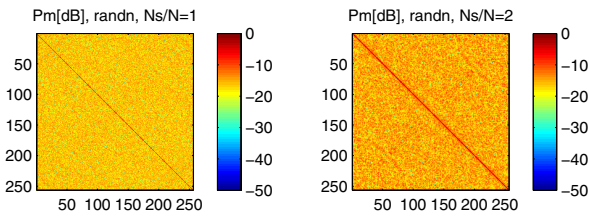


Fig. 3. $|\mathbf{P}_m|$ (in dB) for a general random Gaussian Φ .

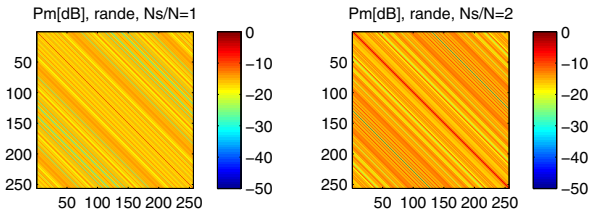


Fig. 4. $|\mathbf{P}_m|$ (in dB) for a random selection Φ .

Then we show an example of the estimated MVDR spectrum using Nyquist-rate signals and compressed signals (with different Φ 's) when the SNR is 3 dB. Figures 5 and 6 correspond to $N_s/N = 1$ and 2, respectively. We plot a normalized version of (20) to make the mean of the estimated spectrum equal to the true spectrum, i.e., $\tilde{P}_y(\omega_i)Q/(Q - M + 1)$ for compressed signals, and $\tilde{P}_x(\omega_i)Q/(Q - N + 1)$ for Nyquist-rate signals, where $\tilde{P}_x(\omega_i)$ is obtained by setting $\Phi = \mathbf{I}_N$ in (20). For Nyquist-rate signals and compressed signals with a Toeplitz Φ , the signal leakage is negligible at noise-only frequencies and the estimated noise floor is about the same level as the noise power σ_n^2 , i.e., 0 dB. For compressed signals

with a non-Toeplitz compression matrix, the signal leakage affects all the frequencies and the estimated noise floor is shifting up by a constant level depending on the signal power, the spectral smoothing ratio N_s/N , and the compression ratio M/N .

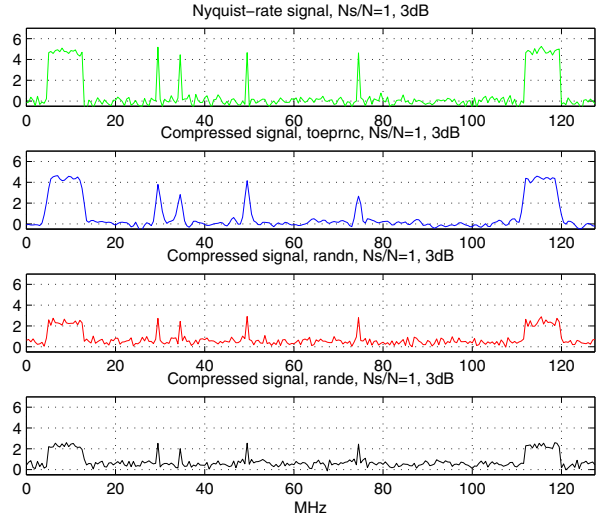


Fig. 5. $N_s/N = 1$. a) Nyquist-rate signal. b) Toeplitz random Gaussian Φ . c) general random Gaussian Φ . d) random selection Φ .

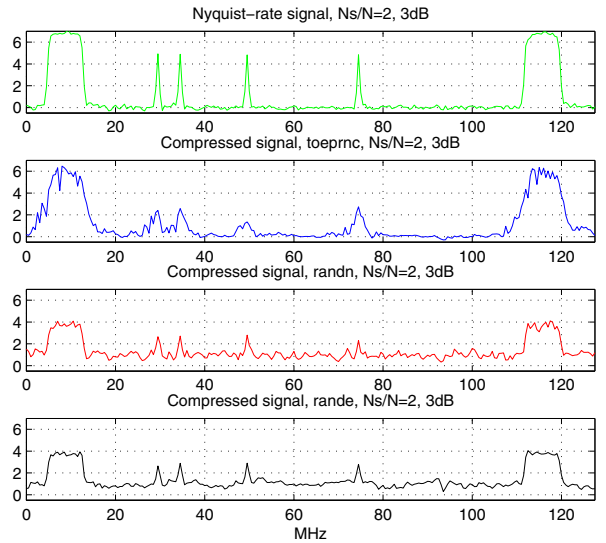


Fig. 6. $N_s/N = 2$. a) Nyquist-rate signal. b) Toeplitz random Gaussian Φ . c) general random Gaussian Φ . d) random selection Φ .

In Figure 7, we plot the cumulative distribution function (CDF) of the estimated noise floor when $N_s/N = 2$. The upper subplot is for an SNR of 0 dB and the lower for an SNR of -5 dB. The estimated noise floor samples are obtained using (20) at noise-only frequencies that are 10 frequencies away from the active frequencies. In both subplots, the thinner

lines are for Nyquist-rate signals, and the thicker lines are for compressed signals. We also plot the theoretical Chi-square CDF curves (solid lines) for reference, i.e., $\chi_{2(Q-N+1)}^2$ for Nyquist-rate signals and $\chi_{2(Q-M+1)}^2$ for compressed signals. Note that the theoretical Chi-square CDF values are calculated assuming $[\mathbf{P}_s]_{i,i} = 0$ in (21). We can see that the estimated noise floor samples follow quite well the theoretical Chi-square curves for Nyquist-rate signals (thinner dashed lines) and compressed signals with a Toeplitz Φ (thicker dashed lines). For compressed signals with either a general random Gaussian Φ (thicker dash-dotted lines) or with a random selection Φ (thicker dotted lines), the mean of the estimated noise floor is shifted towards right (increased) compared to the theoretical Chi-square curves because the signal leakage term $[\mathbf{P}_s]_{i,i}$ is no longer zero and increases with SNR.

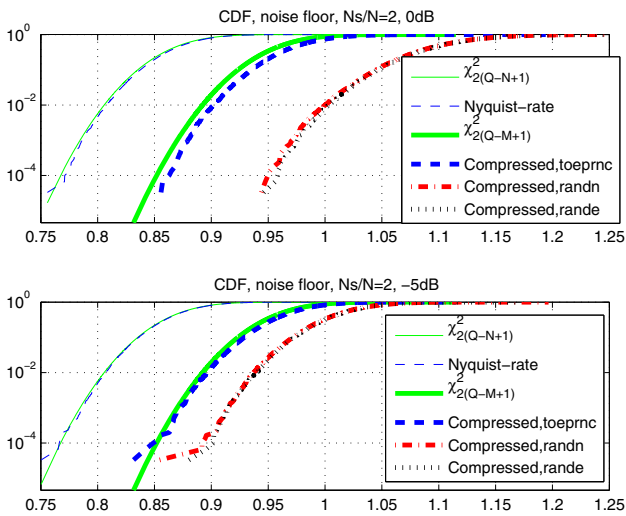


Fig. 7. CDF of the estimated noise floor with spectral smoothing ($N_s/N = 2$). a) SNR=0 dB. b) SNR=-5 dB.

VI. CONCLUSION

We have proposed a CS based MVDR estimator using compressed signals from an AIC for wideband spectrum sensing. The computational complexity of the proposed estimator is considerably less than the conventional CS reconstruction algorithms. There are also cases when conventional l_1 -norm minimization based reconstruction algorithms completely fail, while the CS MVDR approach still gives a reasonable spectrum estimate. For example, in our simulation section when spectral smoothing is used, AIC has a small-sized Φ ($N = 128$, $M = 38$) that is unable to reconstruct the signal of $K = 36$. In order to design a detection threshold, we obtained the probability distribution of the estimated spectrum considering finite samples. We also found that a compression matrix with a Toeplitz structure results in least signal leakage, compared to other choices.

- [1] J. Capon, "High-resolution frequency-wavenumber spectrum analysis", *Proc. IEEE*, Vol. 57, No. 8, pp. 1408-1418, 1969.
- [2] J. Capon and N. R. Goodman, "Probability distributions for estimators of the frequency-wavenumber spectrum", *Proc. IEEE*, Vol. 58, pp. 1785-1786, 1970.
- [3] S. F. Cotter, B. D. Rao, K. Engan, and K. K-Delgado, "Sparse Solutions to Linear Inverse Problems with Multiple Measurement Vectors," *IEEE Trans. on Signal Processing*, vol. 53, pp. 2477-2488, July 2005.
- [4] D. Donoho, "Compressed sensing", *IEEE Trans. on Information Theory*, pp. 1289-1306, Apr. 2006.
- [5] Federal Communications Commission - First Report, and Order and Further Notice of Proposed Rulemaking, "Unlicensed operation in the TV broadcast bands," *FCC 06-156*, Oct. 2006.
- [6] N. R. Goodman, "Statistical analysis based on a certain multivariate complex Gaussian distribution. (An introduction)", *Ann. Math. Statist.*, pp. 152-177, 1963.
- [7] J. Laska, S. Kirolos, Y. Massoud, R. Baraniuk, A. Gilbert, M. Iwen, and M. Strauss, "Random sampling for analog-to-information conversion of wideband signals," *IEEE Dallas Circuits and Systems Workshop*, pp. 119-122, Oct. 2006.
- [8] R. A. Horn and C. R. Johnson, *Matrix Analysis*, Cambridge University Press, Cambridge, 1985.
- [9] K. V. Mardia, J. T. Kent and J. M. Bibby, *Multivariate Analysis*, Academic Press, 1979.
- [10] Y. Wang, G. Leus, and A. Pandharipande, "Direction estimation using compressive sampling array processing", *IEEE Workshop on Statistical Signal Processing*, pp. 626-629, 2009.